Geomechanics and Engineering, *Vol. 10, No. 2 (2016) 189-205*
DOI: http://dx.doi.org/10.12989/gae.2016.10.2.189

Shear stresses below the rectangular foundations subjected to biaxial bending

Ugur Dagdeviren*

Department of Civil Engineering, Dumlupinar University, 43100, Kutahya, Turkey

(*Received June 23, 2015, Revised December 07, 2015, Accepted December 10, 2015*)

Abstract. Soils are subjected to additional stresses due to the loads transferred by the foundations of the buildings. The distribution of stress in soil has great importance in geotechnical engineering projects such as stress, settlement and liquefaction analyses. The purpose of this study is to examine the shear stresses on horizontal plane below the rectangular foundations subjected to biaxial bending on an elastic soil. In this study, closed-form analytical solutions for shear stresses in x and y directions were obtained from Boussinesq's stress equations. The expressions of analytical solutions were simplified by defining the shear stress influence values (I_1, I_2, I_3), and solution charts were presented for obtaining these values. For some special loading conditions, the expressions for shear stresses in the soil below the corners of a rectangular foundation were also given. In addition, a computer program was developed to calculate the shear stress increment at any point below the rectangular foundations. A numerical example for illustrating the use of the presented solution charts was given and, finally, shear stress isobars were obtained for the same example by a developed computer program. The shear stress expressions obtained in this work can be used to determine monotonic and cyclic behavior of soils below rectangular foundations subjected to biaxial bending.

Keywords: shear stress; rectangular foundations; biaxial bending; analytical solution; numerical solution

1. Introduction

When the soils are subjected to external loads due to buildings, embankments or excavations, the stress distribution in soil changes. Stresses applied to the soil by the external loads are not constant under and around the structure and they also vary with the depth. The distribution of stress in soil due to surface loads has a great importance in geotechnical engineering. It is often necessary to calculate the stresses at different depths in foundation analysis and design. For example, to calculate the foundation settlement, the estimation of the vertical stress increment in the soil mass due to net foundation load is required. In foundation design procedure, it is essential to check that the shear stresses induced from the foundation loads must not exceed the shear strength of the soil. Hence, the calculation of the shear stresses below the foundation is required.

The other problem in geotechnical engineering is the presence of the initial static shear stress on horizontal planes below the foundations and in earth structures such as slopes, dams and embankments (Arangelovski and Towhata 2004, Ishibashi *et al*. 1985). Dagdeviren *et al*. (2012),

*Corresponding author, Assistant Professor, Ph.D., E-mail: ugur.dagdeviren@dpu.edu.tr

http://www.techno-press.org/?journal=gae&subpage=7 ISSN: 2005-307X (Print), 2092-6219 (Online)

Keyhani and Haeri (2013) showed the effect of anisotropic consolidation on monotonic undrained behavior of clay and silty sand. Hyodo *et al*. (1994) and Song (2003) examined the undrained monotonic and cyclic loading behavior of clay and silt soils subjected to static shear stress. Vaid and Chern (1983), Uchida and Hasegawa (1986), Hyodo *et al*. (1991), Rahhal and Lefebvre (2000), Vaid *et al*. (2001), Sivathayalan and Ha (2011), Yang and Sze (2011) and Chiaro *et al*. (2012) were investigated the influence of the initial static shear stress on liquefaction resistance of sandy soils by using isotropically and anisotropically consolidated specimens. Seed (1983) developed the K_α correction factor to represent the effect of initial static shear stress on liquefaction resistance. Then, Boulanger (2003) presented reasonable and practical guideline for describing the combined effects of relative density and confining stress on K_α correction factor. Recently, the existing proposals for determination of the K_α correction factor were examined with new data sets covering a wide range of relative densities, confining stresses and static shear stress levels by Yang *et al*. (2013). The results of these studies showed that presence of the initial static shear stress significantly affects the behavior of soils under dynamic loading. Therefore, it is very important to calculate the shear stresses below the foundation of the structures prior to the dynamic analysis.

In geotechnical engineering, the induced stresses from foundation pressures are generally determined by Boussinesq's equations based on the theory of elasticity. Under the assumptions of semi-infinite, weightless, isotropic, homogeneous and elastic half-space soil, Boussinesq (1885) presented a mathematical solution for obtaining the stress distribution resulting from vertical point loading on the soil surface. Although natural soil deposits generally are not fully elastic, isotropic or homogeneous, calculations for estimating the vertical stress distribution give fairly good results for practical purposes. Therefore, the Boussinesq's solutions are widely used to obtain the stresses induced from foundation loads for all types of soils (Das 2010, Algin and Algin 2009).

As the structure loads are transferred to the soil through foundations, the stress equations given for a point load are not realistic in many civil engineering problems. However, the stresses at any depth under the foundations having different geometry (circular, rectangular, strip, triangular, trapezoidal etc.) and different loading types (uniform, triangular, parabolic etc.) can be obtained by integrating Boussinesq's solution over the loaded area. In the literature, although the closed-form solutions for vertical stress for different geometric shapes of loaded areas were presented by various authors (Newmark 1935, Gray 1943, Jarquio and Jarquio 1984, Vitone and Valsangkar 1986, Algin 2000, Wang and Liao 2002), the shear stress solutions are limited with uniformly loaded strip, circular and rectangular foundations (Poulos and Davis 1974, Dagdeviren and Gunduz 2011). However, the foundations are generally subjected to eccentric loading. In such cases, the pressure distribution under the foundation is not uniform. The base stress distributions under the foundations may have triangular or trapezoidal forms depending on the one-way or two-way eccentricity.

In this study, the closed-form exact analytical solutions for the shear stresses (τ_{zx}, τ_{zy}) in *x* and *y* directions on a horizontal plane below the rectangular foundation subjected to biaxial bending (two-way eccentricity) were presented. In order to facilitate the applicability of the shear stress expressions obtained from the analytical solution, shear stress influence values were proposed and presented as solution charts. The shear stress expressions can be only used to calculate the shear stresses below the corners of the rectangular foundation. The shear stress formulas for some special stress conditions such as uniformly loaded, triangular loaded (linearly varying in *x* and *y* directions) and having a zero loaded corner rectangular foundation were presented. Additionally, a computer program was developed to calculate the shear stresses at any point below the foundation based on numerical integration method. A numerical example for illustrating the use of the

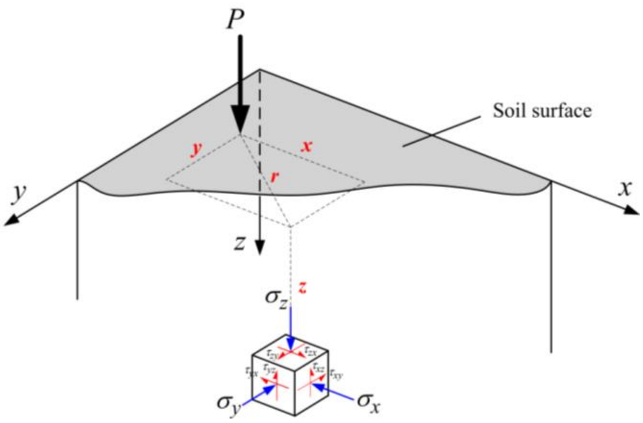

Fig. 1 Positive stresses on the soil element due to vertical point load

presented solution charts was given and, finally, shear stress isobars were obtained for the same example by a developed computer program.

2. Derivation

According to Boussinesq's solution, the shear stresses resulting from a vertical point load on soil surface are shown in Fig. 1 on a soil element. The sign of shear stresses shown in this figure is positive and they are defined as

$$\tau_{zx} = \frac{3Pxz^2}{2\pi(x^2 + y^2 + z^2)^{5/2}} \tag{1a}$$

$$\tau_{zy} = \frac{3Pyz^2}{2\pi(x^2 + y^2 + z^2)^{5/2}} \tag{1b}$$

When a rectangular foundation with B and L dimensions along the x and y directions, respectively, is subjected to biaxial bending moments, then the base stresses at the corners of the foundation (q_A; q_B; q_C; q_D) differ from each other. The typical distribution of the base stresses under the rectangular foundation subjected to biaxial bending moments is shown in Fig. 2. Since base stress distribution is linear, then the base stress distribution can be expressed as

$$q = q_A\left(1 - \frac{x}{k} - \frac{y}{t}\right) \tag{2}$$

where k and t are run-out distances of linearly distributed stress function along the x and y directions, respectively. k and t are given by

$$k = \frac{B.q_A}{q_A - q_B} \tag{3a}$$

$$t = \frac{L.q_A}{q_A - q_C} \tag{3b}$$

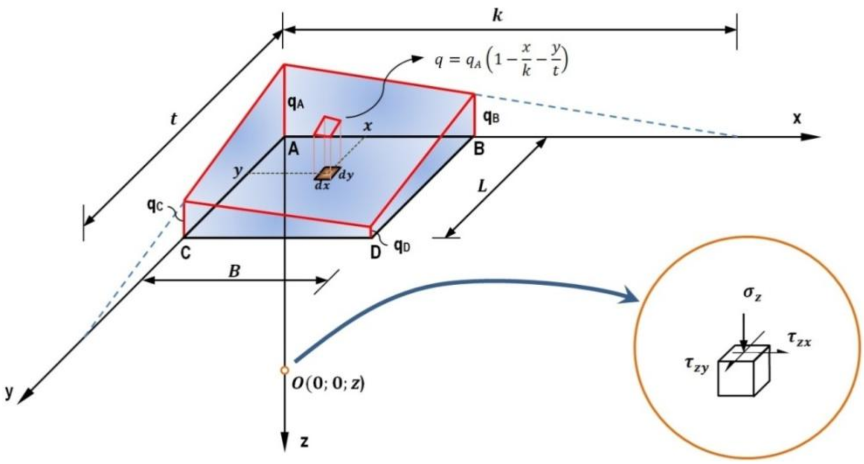

Fig. 2 Eccentrically loaded rectangular foundation

If q_A is less than q_B or q_C, then k or t can be negative.

If the rectangular foundation is divided into infinitesimally small areas, then the small point load $(q.dA)$ acting on this small area can be substituted into Eq. (1a), giving shear stress (τ_{zx}) under the rectangular foundation. Similarly, all the other small loads acting on the other infinitesimally small areas also produce shear stresses (τ_{zx}) under the rectangular foundation. Therefore, in order to calculate the total shear stress (τ_{zx}) at any point under the rectangular foundation, the double integration over the rectangular foundation area is calculated as

$$\tau_{zx} = \iint_A \frac{3xz^2q}{2\pi(x^2+y^2+z^2)^{5/2}}dA \tag{4}$$

The exact analytical solution for the shear stress τ_{zx} which is in x direction on x-y plane at depth z beneath the origin (point A in Fig. 2) is given by

$$(\tau_{zx})_A = (-)\frac{q_A}{2\pi}.\left\{\begin{array}{c} \left(\dfrac{L}{(L^2+z^2)^{\frac{1}{2}}} - \dfrac{Lz^2}{(B^2+z^2)(B^2+L^2+z^2)^{\frac{1}{2}}}\right) \\ +\dfrac{z}{t}\left(\dfrac{z}{(L^2+z^2)^{\frac{1}{2}}} + \dfrac{z}{(B^2+z^2)^{\frac{1}{2}}} - \dfrac{z}{(B^2+L^2+z^2)^{\frac{1}{2}}} - 1\right) \\ +\dfrac{z}{k}\left(\dfrac{BLz-(B^2+z^2)(B^2+L^2+z^2)^{1/2}\arctan\left(\dfrac{BL}{z(B^2+L^2+z^2)^{1/2}}\right)}{(B^2+z^2)(B^2+L^2+z^2)^{1/2}}\right) \end{array}\right\} \tag{5}$$

To simplify Eq. (5), the foundation dimensions B and L are normalized by using depth z as $m = B/z$; $n = L/z$. Using k, t definitions given in Eqs. (3a) and (3b) and also using m and n definitions in Eq. (5), the expression becomes

$$(\tau_{zx})_A = (-)q_A\left[I_1 + \left(1-\frac{q_C}{q_A}\right)I_2 + \left(1-\frac{q_B}{q_A}\right)I_3\right] \tag{6}$$

where I_1, I_2, I_3 are called influence values for shear stress in *x* direction on *x-y* plane (Fig. 2) and are defined by

$$I_1 = \frac{n}{2\pi}\left[\frac{1}{(1+n^2)^{1/2}} - \frac{1}{(1+m^2)(1+m^2+n^2)^{1/2}}\right] \tag{7a}$$

$$I_2 = \frac{1}{2\pi n}\left[\frac{1}{(1+m^2)^{1/2}} + \frac{1}{(1+n^2)^{1/2}} - \frac{1}{(1+m^2+n^2)^{1/2}} - 1\right] \tag{7b}$$

$$I_3 = \frac{1}{2\pi m}\left[\frac{mn}{(1+m^2)(1+m^2+n^2)^{1/2}} - \arctan\left(\frac{mn}{(1+m^2+n^2)^{1/2}}\right)\right] \tag{7c}$$

The shear stress influence values in Eq. (7) are functions of m and n values. Moreover, these influence values are independent from the stress distribution function and base stress intensity. In order to facilitate the applicability of the formulas, solution charts for I_1, I_2, I_3 influence values have been presented in Figs. 3, 4 and 5, respectively. The solution charts for these influence values are similar to the vertical stress increment chart presented by Fadum (1948). These charts are simple and easily applicable to geotechnical engineering applications.

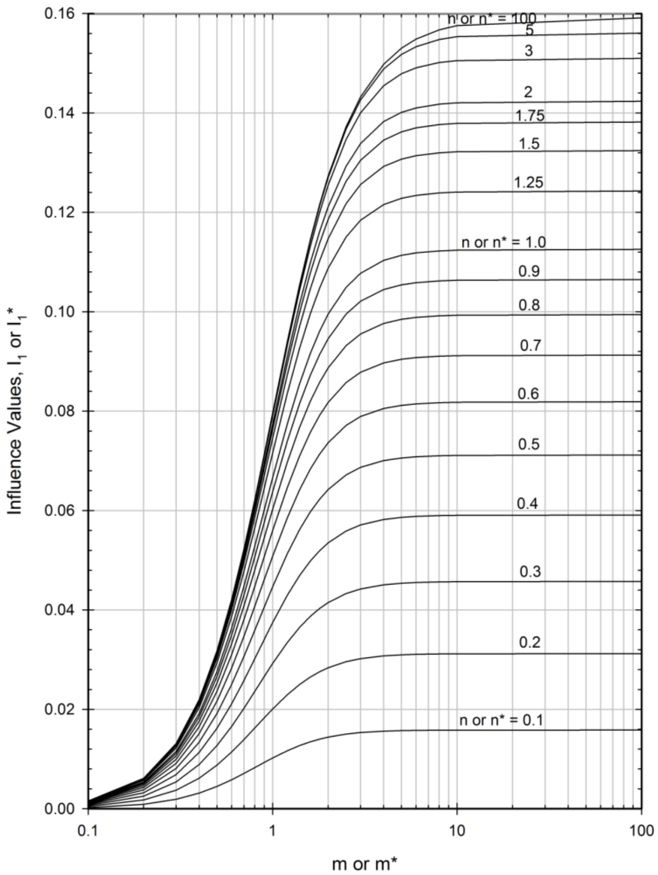

Fig. 3 Shear stress influence values (I_1, I_1^*)

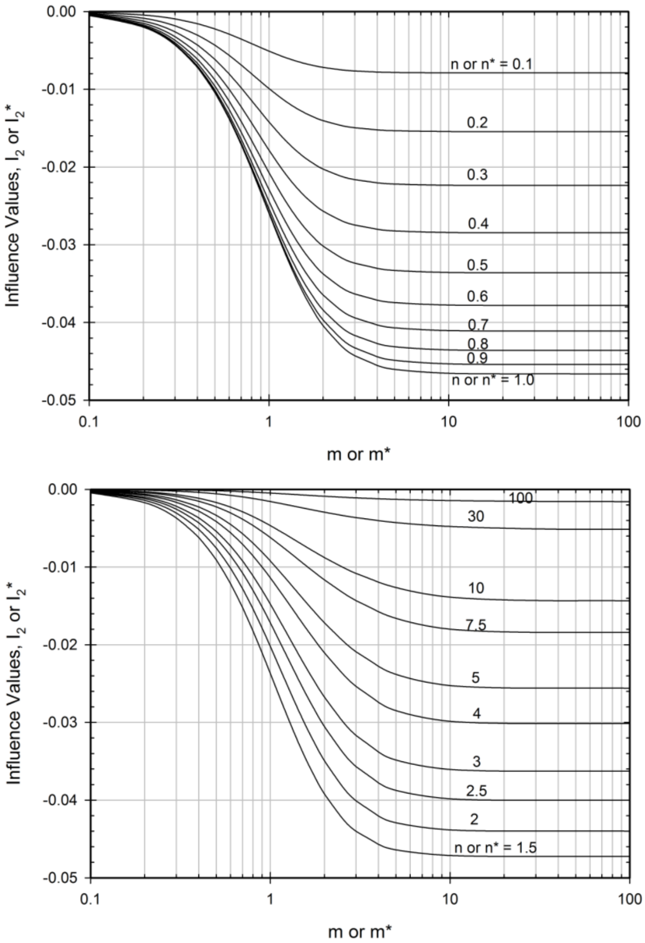

Fig. 4 Shear stress influence values (I_2, I_2^*)

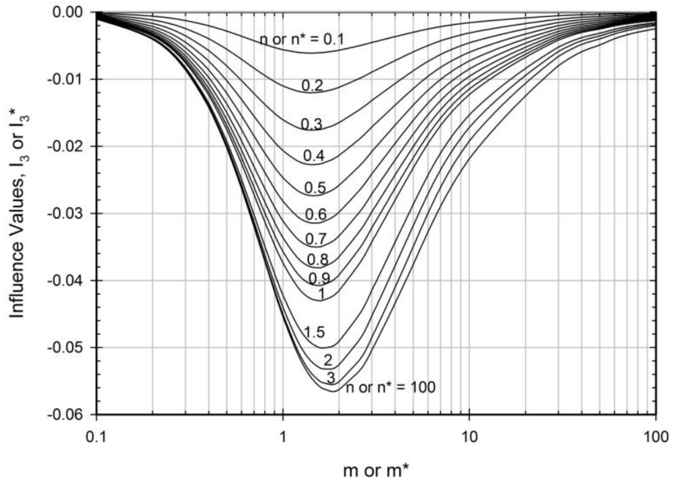

Fig. 5 Shear stress influence values (I_3, I_3^*)

Similarly, the shear stresses at any depth below the other corner points of the rectangular foundation are obtained from Eqs. (8)-(10).

$$(\tau_{zx})_B = q_B\left[I_1 + \left(1 - \frac{q_D}{q_B}\right)I_2 + \left(1 - \frac{q_A}{q_B}\right)I_3\right] \tag{8}$$

$$(\tau_{zx})_C = (-)q_C\left[I_1 + \left(1 - \frac{q_A}{q_C}\right)I_2 + \left(1 - \frac{q_D}{q_C}\right)I_3\right] \tag{9}$$

$$(\tau_{zx})_D = q_D\left[I_1 + \left(1 - \frac{q_B}{q_D}\right)I_2 + \left(1 - \frac{q_C}{q_D}\right)I_3\right] \tag{10}$$

When similar operations are applied to shear stresses in y direction on x-y plane, the shear stress under the corner point A shown in Fig. 2 is calculated by

$$(\tau_{zy})_A = (-)\frac{q_A}{2\pi}\cdot\left\{\begin{array}{c}\left(\dfrac{B}{(B^2+z^2)^{\frac{1}{2}}} - \dfrac{Bz^2}{(L^2+z^2)(B^2+L^2+z^2)^{\frac{1}{2}}}\right)\\ +\dfrac{z}{k}\left(\dfrac{z}{(B^2+z^2)^{\frac{1}{2}}} + \dfrac{z}{(L^2+z^2)^{\frac{1}{2}}} - \dfrac{z}{(B^2+L^2+z^2)^{\frac{1}{2}}} - 1\right)\\ +\dfrac{z}{t}\left(\dfrac{BLz - (L^2+z^2)(B^2+L^2+z^2)^{1/2}\arctan\left(\dfrac{BL}{z(B^2+L^2+z^2)^{1/2}}\right)}{(L^2+z^2)(B^2+L^2+z^2)^{1/2}}\right)\end{array}\right\} \tag{11}$$

If the foundation dimensions are normalized by depth z as, $m^* = L/z$ and $n^* = B/z$, then Eq. (11) is simplified. The shear stresses in y direction on x-y plane at any depth below the corner points of the rectangular foundation (Fig. 2) can be summarized as

$$(\tau_{zy})_A = (-)q_A\left[I_1^* + \left(1 - \frac{q_B}{q_A}\right)I_2^* + \left(1 - \frac{q_C}{q_A}\right)I_3^*\right] \tag{12a}$$

$$(\tau_{zy})_B = (-)q_B\left[I_1^* + \left(1 - \frac{q_A}{q_B}\right)I_2^* + \left(1 - \frac{q_D}{q_B}\right)I_3^*\right] \tag{12b}$$

$$(\tau_{zy})_C = q_C\left[I_1^* + \left(1 - \frac{q_D}{q_C}\right)I_2^* + \left(1 - \frac{q_A}{q_C}\right)I_3^*\right] \tag{12c}$$

$$(\tau_{zy})_D = q_D\left[I_1^* + \left(1 - \frac{q_C}{q_D}\right)I_2^* + \left(1 - \frac{q_B}{q_D}\right)I_3^*\right] \tag{12d}$$

where

$$I_1^* = \frac{n^*}{2\pi}\left[\frac{1}{(1+n^{*2})^{\frac{1}{2}}} - \frac{1}{(1+m^{*2})(1+m^{*2}+n^{*2})^{\frac{1}{2}}}\right] \tag{13a}$$

$$I_2^* = \frac{1}{2\pi n^*}\left[\frac{1}{(1+m^{*2})^{1/2}} + \frac{1}{(1+n^{*2})^{1/2}} - \frac{1}{(1+m^{*2}+n^{*2})^{1/2}} - 1\right] \tag{13b}$$

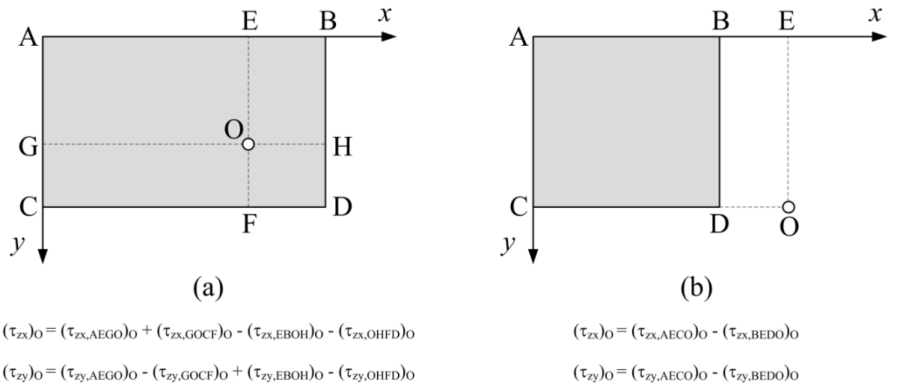

Fig. 6 Superposition examples for shear stress calculations at point O

$$I_3^* = \frac{1}{2\pi m^*}\left[\frac{m^* n^*}{(1+m^{*2})(1+m^{*2}+n^{*2})^{1/2}} - \arctan\left(\frac{m^* n^*}{(1+m^{*2}+n^{*2})^{1/2}}\right)\right] \tag{13c}$$

When Eqs. (7) and (13) are noticed, it is seen that m^* and n^* expressions are used instead of m and n expressions in the equations, respectively. Thus, the solution charts in Figs. 3-5 can be used to determine the shear stress in both the x and y directions on horizontal plane. If m and n are used, then I_1, I_2, I_3 influence values are obtained; if m^* and n^* are used, then I_1^*, I_2^*, I_3^* influence values are obtained from solution charts.

The expressions presented above give the shear stresses at any depth below the corners of the rectangular foundation. In case when the shear stress is desired at any other point, then the loaded area is divided into some other rectangular parts as shown in Fig. 6. The shear stresses below the corresponding corners are determined for each rectangular part and then net shear stress can be calculated by using the superposition rule. This procedure is similar to the calculation procedure of the vertical normal stress based on Newmark's solution. However, during the superposition of shear stress values, the directions of shear stresses must be taken into account. The calculation procedure of the shear stress below the O-point inside ABCD rectangular loaded area is shown in Fig. 6(a). In order to obtain the shear stresses below the O-point, ABCD loaded area is divided to the four rectangular loaded areas. The shear stresses in x direction below point O, which are induced by AEGO and GOCF loaded areas, have positive sign; whereas the those induced by EBOH and OHFD loaded areas have negative signs. The net shear stress at point O can be evaluated by adding the shear stresses contributed by the four rectangular loaded areas as shown in Fig. 6(a). The calculation of the shear stress at any point outside the ABCD loaded area is given in Fig. 6(b). In this case, AECO rectangular area is assumed to be the loaded area, whereas BEDO rectangular area is assumed to be the unloaded area. Thus, the net shear stress at O-point is calculated as shown in Fig. 6(b).

3. Shear stresses for special stress conditions under the rectangular foundations

3.1 Uniformly loaded rectangular foundations

If the flexible rectangular foundation is only subjected to the vertical load, the base stresses under the corners of the rectangular foundation ($q_A = q_B = q_C = q_D = q$) are equal and the foundation becomes uniformly loaded rectangular foundation as shown in Fig. 7(a). For the uniformly loaded rectangular foundations, the factors of I_2 and I_3 defined in Eqs. (6), (8)-(10) and the factors of I_2^* and I_3^* defined in Eq. (12) become zero. At this situation, the shear stress expressions given in Eqs. (6) and (12a) transform to Eqs. (14a) and (14b). The shear stress formulas for the points beneath the other corner points of the rectangular foundation are summarized in Table 1 and 2.

$$(\tau_{zx})_A = (-)q \times I_1 \tag{14a}$$

$$(\tau_{zy})_A = (-)q \times I_1^* \tag{14b}$$

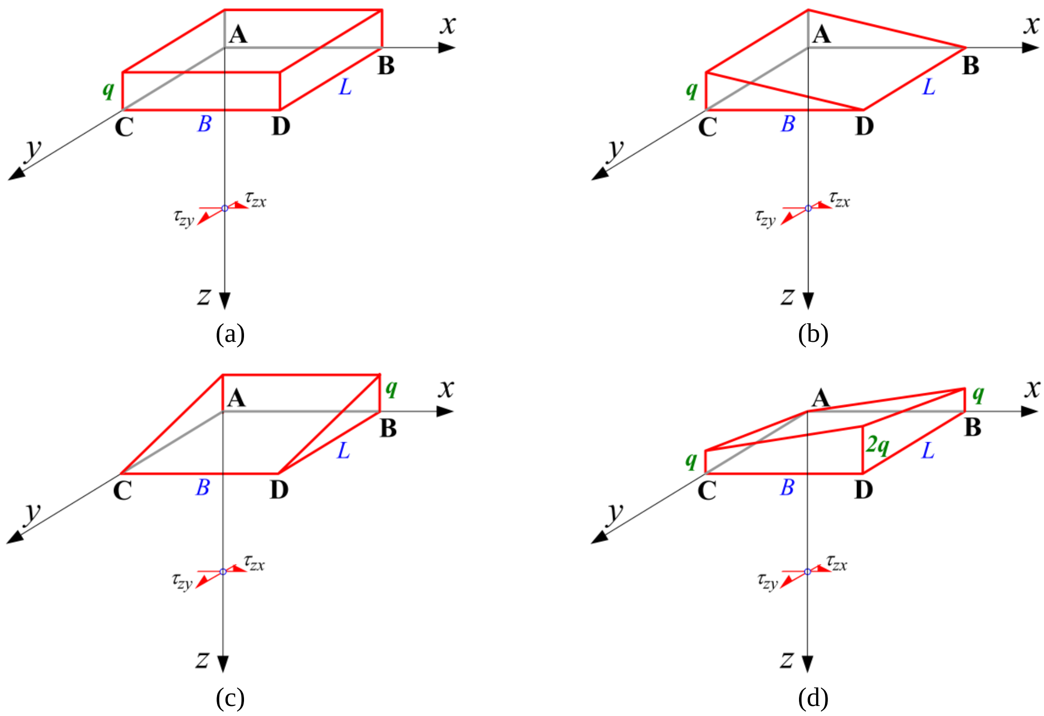

Fig. 7 Special stress conditions

Table 1 Shear stresses in *x*-direction beneath the corners for different loading types (τ_{zx})

Shear stress in *x*-direction	Loading type			
	3.1 Uniformly loaded (Fig. 7(a))	3.2 Triangularly loaded (*x*-direction) (Fig. 7(b))	3.3 Triangularly loaded (*y*-direction) (Fig. 7(c))	3.4 Zero-loaded corner (Fig. 7(d))
$(\tau_{zx})_A$	$(-)q \times I_1$	$(-)q \times (I_1 + I_3)$	$(-)q \times (I_1 + I_2)$	$(-) - q \times (I_2 + I_3)$
$(\tau_{zx})_B$	$q \times I_1$	$-q \times I_3$	$q \times (I_1 + I_2)$	$q \times (I_1 - I_2 + I_3)$
$(\tau_{zx})_C$	$(-)q \times I_1$	$(-)q \times (I_1 + I_3)$	$(-) - q \times I_2$	$(-)q \times (I_1 + I_2 - I_3)$
$(\tau_{zx})_D$	$q \times I_1$	$-q \times I_3$	$-q \times I_2$	$q \times (2I_1 + I_2 + I_3)$

Table 2 Shear stresses in y-direction beneath the corners for different loading types (τ_{zy})

Shear stress in y-direction	Loading type			
	3.1 Uniformly loaded (Fig. 7(a))	3.2 Triangularly loaded (x-direction) (Fig. 7(b))	3.3 Triangularly loaded (y-direction) (Fig. 7(c))	3.4 Zero-loaded corner (Fig. 7(d))
$(\tau_{zy})_A$	$(-)q \times I_1^*$	$(-)q \times (I_1^* + I_2^*)$	$(-)q \times (I_1^* + I_3^*)$	$(-) - q \times (I_2^* + I_3^*)$
$(\tau_{zy})_B$	$(-)q \times I_1^*$	$(-) - q \times I_2^*$	$(-)q \times (I_1^* + I_3^*)$	$(-)q \times (I_1^* + I_2^* - I_3^*)$
$(\tau_{zy})_C$	$q \times I_1^*$	$q \times (I_1^* + I_2^*)$	$-q \times I_3^*$	$q \times (I_1^* - I_2^* + I_3^*)$
$(\tau_{zy})_D$	$q \times I_1^*$	$-q \times I_2^*$	$-q \times I_3^*$	$q \times (2I_1^* + I_2^* + I_3^*)$

The expressions in Eqs. (14a) and (14b) are equal to the shear stress expressions given by Dagdeviren and Gunduz (2011). So, the solution obtained for the uniformly loaded rectangular foundation is a special case of the general shear stress expressions given in Eqs. (6), (8)-(10) and (12).

3.2 Triangularly loaded rectangular foundations (*Linearly varying in x-direction*)

If the flexible rectangular foundation is subjected to positive bending moment in y-direction (M_y) and vertical load (P) such that $M_y/P = B/6$, then for the foundation becomes the triangularly loaded rectangular foundation (linearly decreasing in x-direction) as shown in Fig. 7(b). For this rectangular foundation, the base stresses under the corner points are defined as

$$q_A = q_C = q \qquad \text{and} \qquad q_B = q_D = 0 \tag{15}$$

In order to determine the shear stresses in x-direction below the corner points Eqs. (6) and (8)-(10) can be used. For this case, the factor of the I_2 influence value becomes zero and the factor of the I_3 influence value becomes 1. For this case, the basic shear stress expressions transform to those shown in Table 1. For this rectangular foundation problem, the shear stresses in y-direction beneath the corner points can be calculated by the equations given in Table 2.

3.3 Triangularly loaded rectangular foundations (*Linearly varying in y-direction*)

If the flexible rectangular foundation is subjected to negative bending moment in x-direction (M_x) and a vertical load (P) such that $|M_x/P|$ = L/6, then for this case, the foundation becomes the triangularly loaded rectangular foundation (linearly decreasing in y-direction) as shown in Fig. 7(c). For this rectangular foundation, the base stresses under the corner points are defined as

$$q_A = q_B = q \qquad \text{and} \qquad q_C = q_D = 0 \tag{16}$$

For this rectangular foundation problem, the shear stresses in x-direction and y-direction below the corner points can be calculated by equations given in Tables 1 and 2, respectively.

3.4 Rectangular foundations with a zero-loaded corner

If the flexible rectangular foundation is subjected to a positive bending moment in x-direction (M_x) and a negative bending moment in y-direction (M_y) in addition to a vertical load (P) such that $|M_y/P|$ = B/12 and M_x/P = L/12, then the foundation load increases in x and y directions as shown in Fig. 7(d) (Vitone and Valsangkar 1986). In this stress condition, the base stress at corner point A is zero, base stresses at corners B and C are equal to q, and base stress at corner D is equal to $2q$.

$$q_A = 0 \qquad \text{and} \qquad q_B = q_C = q \qquad \text{and} \qquad q_D = 2q \tag{17}$$

For this rectangular foundation problem, the shear stresses in x-direction and y-direction below the corner points can be calculated by equations given in Tables 1 and 2, respectively.

4. Numerical solution and computer program

The presented analytical solutions for rectangular foundations can only be used for finding the shear stresses below the corners of loaded area. When the shear stress is desired at any point except the corner of the rectangular foundation, the loaded area must be divided into different rectangular parts. The contribution of each part below the corner point is determined and net shear stress can be calculated by superposition rule. However, that kind of analytical solution are time consuming and numerical integration methods can be used in order to eliminate the disadvantage of the analytical solution.

The simplest numerical integration method is to divide the loaded rectangular area into small areas. In this method, the small equivalent point loads (P_i) acting on these small areas and their effects on the related points are calculated as shown in Fig. 8. Then, net shear stresses (τ_{zx}, τ_{zy}) at any point under the rectangular foundation are determined by superposition rule. The numerical method can be formulated as

$$P_i = q_A\left(1 - \frac{x_i}{k} - \frac{y_i}{t}\right).\frac{BL}{n_e} \tag{18}$$

$$\tau_{zx} = \sum_{i=1}^{n_e} \frac{3P_i.\Delta x_i.(\Delta z_i)^2}{2\pi.(R_i)^5} \tag{19}$$

$$\tau_{zy} = \sum_{i=1}^{n_e} \frac{3P_i.\Delta y_i.(\Delta z_i)^2}{2\pi.(R_i)^5} \tag{20}$$

where n_e is the total number of the small areas, P_i is the equivalent point load acting on small area; x_i and y_i are the x and y coordinates of the centroid of the small area, R_i is the distance between the centroid of the small area and the point which for the stress increment will be calculated.

As the number of the small areas increases, the results obtained with numerical solutions approach to the results of analytical solution. Since Coduto (1999) suggests that the minimum number of the small areas must not be less than 1000, it is decided to use 10000 small areas in

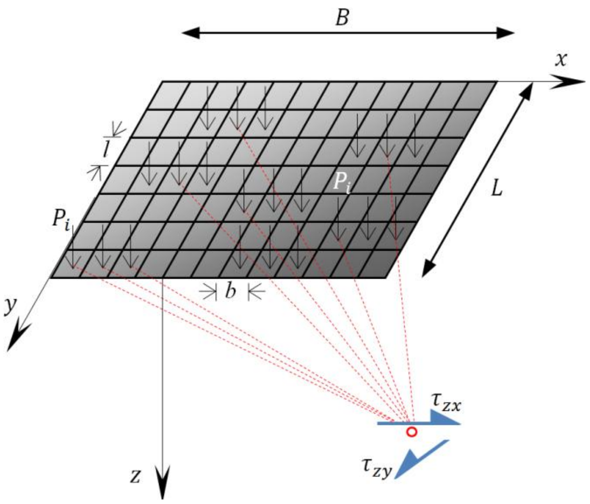

Fig. 8 Numerical integration method

developed computer program. However, this condition is not sufficient especially in order to determine the stress statements in planes close to foundation base ($z = 0$). In this study, the edge lengths of the small elements (b, l) were selected as one-fourth of the R_i as suggested by Stoll (1960). In that case, the differences between the analytical and numerical solutions are expected about 2% (Capper and Cassie 1969).

The stress distribution is generally presented as stress isobars in practice. A stress isobar is a stress contour which connects all points below the ground surface at which the shear stress is the

```
Begin
     Input B, L, qA, qB, qC, qD
     Calculate k, t
     For z=0 to 2.5B (increment 0.05B)
          psx = max (100B; 4B/z)
          psy = max (100L; 4L/z)
          b   = B/psx
          l   = L/psx
          element = psx*psy
          For i = 1 to element
               Calculate xi, yi, Pi
          End for
          For ay = -L to 2L (increment 0.05L)
               For ax = -B to 2B (increment 0.05B)
                    τzx = 0
                    τzy = 0
                    For i = 1 to element
                         Calculate Δxi, Δyi, Ri, τzx,i, τzy,i
                         τzx = τzx + τzx,i
                         τzy = τzy + τzy,i
                    End for
                    Write to report.
                         z; ay; ax; τzx; τzy
               End for
          End for
     End for
End
```

Fig. 9 Pseudocode for computer program

same. The calculation of the shear stress increment at any point with stress isobars is very easy and practical. In order to obtain the stress isobars, the soil mass was divided into 60 parts in the *x* and *y* directions and was divided into 50 parts in the *z* direction. The shear stress increments were calculated at a total of 189771 points. The pseudocode for the computer program is shown in Fig. 9.

5. Numerical example

A numerical example is given to show how the shear stress expressions can be used in calculating the shear stresses at any depth below the corners of the rectangular foundation subjected to biaxial bending.

Problem:

The data for a typical rectangular foundation subjected to biaxial bending as shown in Fig. 2 are given below. The shear stresses in *x*-direction (τ_{zx}) and y-direction (τ_{zy}) below the corners are asked to be calculated at depth z = 4 m.

Foundation dimensions: B = 4 m and L = 6 m
Base stress intensities at the corners: q_A = 200 kPa, q_B = 140 kPa, q_C = 100 kPa, q_D = 40 kPa
Depth: z = 4 m

Solution:

(a) The shear stresses in *x*-direction (τ_{zx}):
Normalized foundation dimensions are

$$m = B/z = \frac{4}{4} = 1.0 \qquad \text{and} \qquad n = L/z = \frac{6}{4} = 1.5$$

For $m = 1.0$ and $n = 1.5$; I_1, I_2, I_3 influence values can be obtained using Eq. (7) or alternatively from the solution charts in Figs. 3, 4 and 5, respectively.

$$I_1 = 0.0745; \qquad I_2 = -0.0237; \qquad I_3 = -0.0422$$

The shear stress in *x*-direction under the corner points *A*, *B*, *C* and *D* can be calculated from Eqs. (6) and (8)-(10).

$$(\tau_{zx})_A = (-)10.00 \text{ kPa}; \qquad (\tau_{zx})_B = 10.60 \text{ kPa};$$

$$(\tau_{zx})_C = (-)7.29 \text{ kPa}; \qquad (\tau_{zx})_D = 7.88 \text{ kPa}$$

(b) The shear stresses in *y*-direction (τ_{zy}):
Normalized foundation dimensions are

$$m^* = L/z = \frac{6}{4} = 1.5; \qquad n^* = B/z = 4/4 = 1.0$$

For $m^* = 1.5$ and $n^* = 1.0$; I_1^*, I_2^*, I_3^* influence values can be obtained using Eq. (13) or alternatively from the solution charts in Figs. 3, 4 and 5, respectively.

$$I_1^* = 0.0888; \qquad I_2^* = -0.0355; \qquad I_3^* = -0.0430$$

The shear stress in *y*-direction under the corners *A*, *B*, *C* and *D* can be calculated from Eq. (12).

$$\left(\tau_{zy}\right)_A = (-)11.33 \text{ kPa}; \qquad \left(\tau_{zy}\right)_B = (-)10.26 \text{ kPa};$$

$$\left(\tau_{zy}\right)_C = 11.05 \text{ kPa}; \qquad \left(\tau_{zy}\right)_D = 9.98 \text{ kPa}$$

Similar calculations can be performed for different depths below the corner points of the sample rectangular foundation. The variation of the shear stresses in the x and y directions with depth are shown in Fig. 10. It is seen from these graphics that the variation of the shear stresses below the corner points are different from each other.

Therefore, this problem was solved by developed computer program. The shear stress values were computed at a total of 189771 points. The stress isobars were plotted at critical planes such as $y = 0,\ y = L/2,\ y = L$ and $x = 0,\ x = B/2,\ x = B$ in Fig. 11. The shear stresses concentrate at the edges of the rectangular foundation. The shear stresses at any point below the rectangular foundation can be easily calculated by shear stress isobars for different planes.

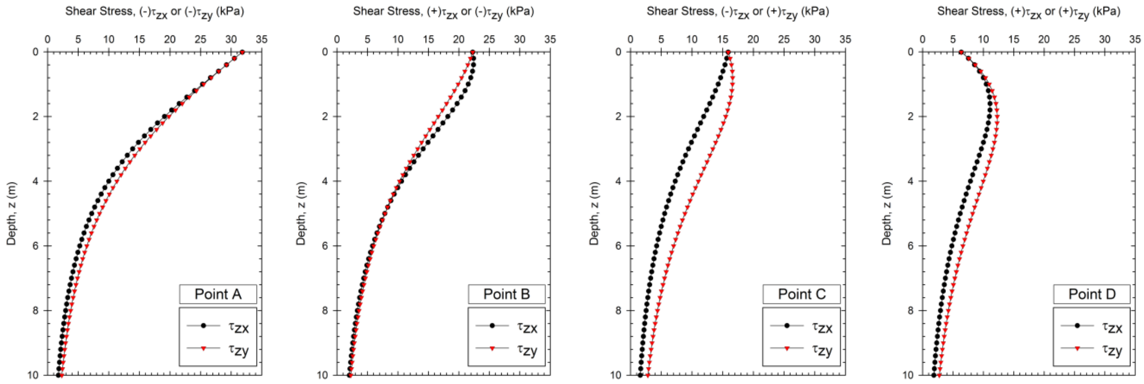

Fig. 10 Shear stress distributions under the corner points of the sample rectangular foundation

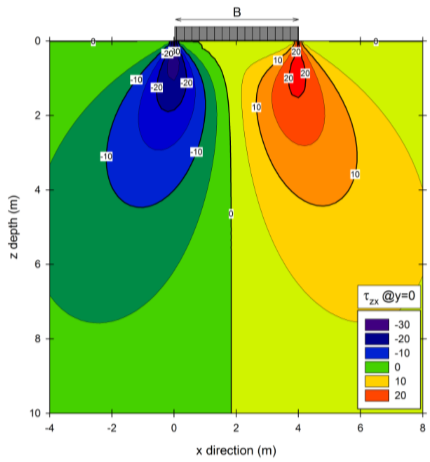

(a)

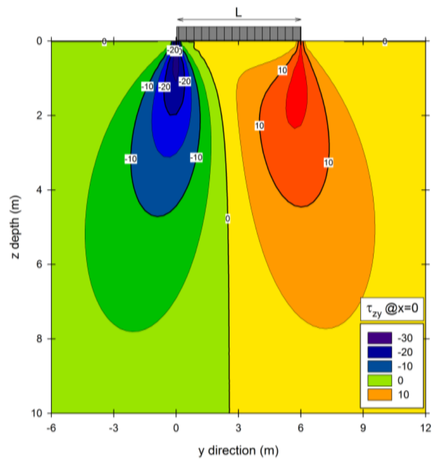

(d)

Fig. 11 Shear stress isobars under the sample rectangular foundation

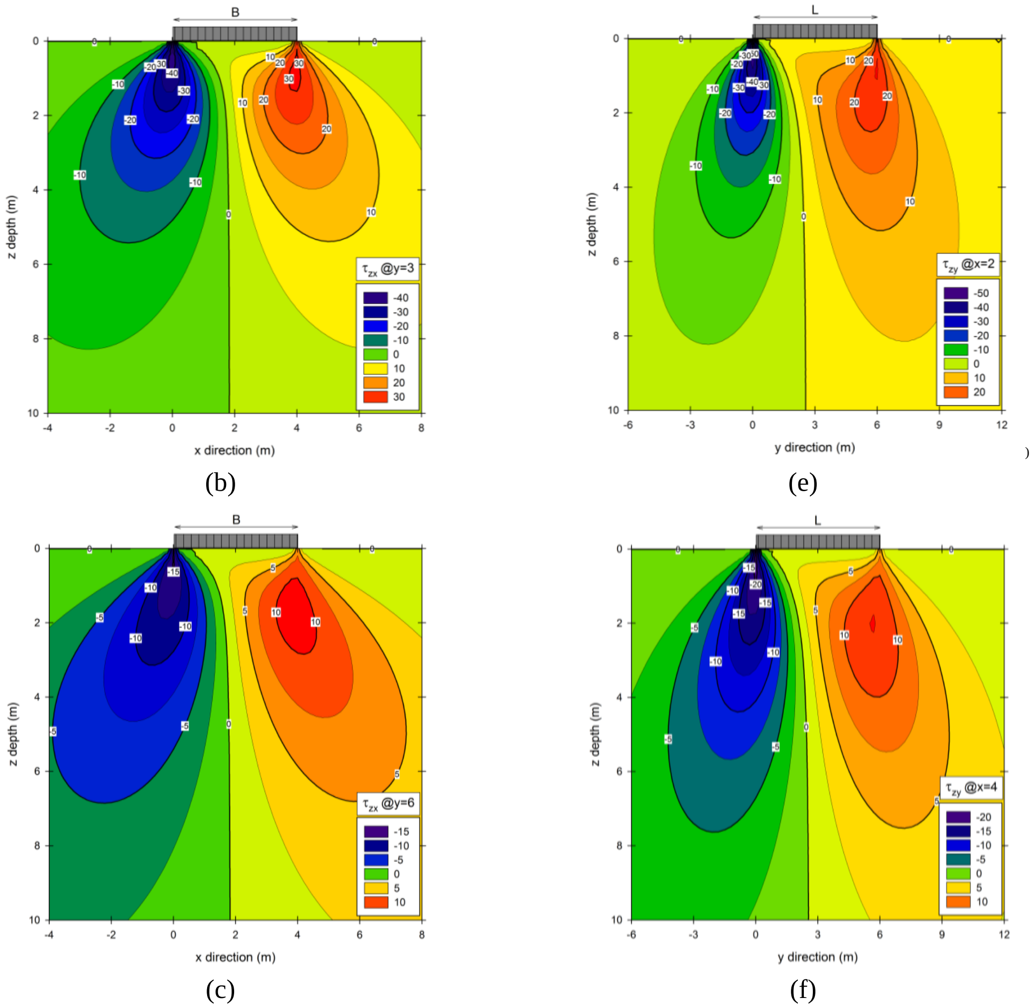

Fig. 11 Continued

6. Conclusions

In this work, closed-form analytical solutions and computer program based on numerical integration method were developed to determine the shear stresses at any point on a horizontal plane of any depth below the eccentrically loaded rectangular foundations. Both analytical and numerical methods used in the study are based on Boussinesq's stress equations. In order to simplify the analytical solutions, the shear stress influence values were defined and were given as solution charts which are simple and applicable for practical uses. The shear stress expressions for the rectangular foundations under some typical stress conditions such as uniformly loaded, triangularly loaded (linearly varying in x and y direction) and the zero loaded corner were obtained using the analytical solutions. A numerical example was given to show how the shear stress expressions can be used in practice. As a result, these analytical and numerical solutions can be used to calculate the shear stresses for various loading types for the eccentrically loaded rectangular foundations.

Acknowledgments

The author is grateful to Prof. Dr. Zeki Gunduz, Prof. Dr. Mustafa Tuncan, Prof. Dr. Mehmet Tevfik Bayer and Prof. Dr. M. Cagatay Karabork for their help during the preparation of the manuscript.

References

Algin, H.M. (2000), "Stresses from linearly distributed pressures over rectangular areas", *Int. J. Numer. Anal. Meth. Geomech.*, **24**(8), 681-692.

Algin, H.M. and Algin, Z. (2009), "Elastic settlements under linear surface pressures on rectangular areas", *Int. J. Numer. Anal. Meth. Geomech.*, **33**(8), 1087-1108.

Arangelovski, G. and Towhata, I. (2004), "Accumulated deformation of sand with initial shear stress and effective stress state lying near failure conditions", *Soils Found.*, **44**(6), 1-16.

Boulanger, R.W. (2003), "Relating *Kα* to relative state parameter index", *J. Geotech. Geoenviron. Eng.*, **129**(8), 770-773.

Boussinesq, J. (1885), *Application des potentials a l'etude de l'equilibre et du mouvement des solides elastiques*, Gauthier-Villars, Paris, France.

Capper, P.L. and Cassie, W.F. (1969), *The Mechanics of Engineering Soils*, (Fifth Edition), Çeviri: (Kumbasar, V., Kip, F.), "İnşaat Mühendisliğinde Zemin Mekaniği", Çağlayan Kitabevi.

Chiaro, G., Junichi, K. and Sato, T. (2012), "Effects of initial static shear on liquefaction and large deformation properties of loose saturated Toyoura sand in undrained cyclic torsional shear tests", *Soils Found.*, **52**(3), 498-510.

Coduto, D.P. (1999), *Geotechnical Engineering*: *Principles and Practices*, Prentice Hall, NJ, USA.

Dagdeviren, U. and Gunduz, Z. (2011), "Calculation of shear stresses under uniformly loaded rectangular foundation", *Proceedings of the 6th International Advanced Technologies Symposium*, Elazig, Turkey, May, pp. 129-134. [In Turkish]

Dagdeviren, U., Gunduz, Z. and Tuncan, M. (2012), "The behavior of clayey soils subjected to initial static shear stress under the monotonic loads", *Proceedings of the 14th National Congress on Soil Mechanics and Foundation Engineering*, Isparta, Turkey, October, pp. 275-284. [In Turkish]

Das, B.M. (2010), *Principles of Geotechnical Engineering*, (7th Edition), Cengage Learning.

Fadum, R.E. (1948), "Influence values for estimating stresses in elastic foundations", *Proceedings of the 2nd International Conference on Soil Mechanics and Foundation Engineering*, Rotterdam, The Netherlands, June, (Volume 3), pp. 77-84.

Gray, H. (1943), "Stresses and displacements from loads over rectangular area", *Civil Engineering*, *ASCE*, **13**(5), 227-229.

Hyodo, M., Murata, H., Yasufuku, N. and Fujii, T. (1991), "Undrained cyclic shear strength and residual shear strain of saturated sand by cyclic triaxial tests", *Soils Found.*, **31**(3), 60-76.

Hyodo, M., Yamamoto, Y. and Sugiyama, M. (1994), "Undrained cyclic shear behaviour of normally consolidated clay subjected to initial static shear stress", *Soils Found.*, **34**(4), 1-11.

Ishibashi, I., Kawamura, M. and Bhatia, S.K. (1985), "Effect of initial shear on cyclic behavior of sand", *J. Geotech. Eng.*, **111**(12), 1395-1410.

Jarquio, R. and Jarquio, V. (1984), "Vertical stress formulas for triangular loading", *J. Geotech. Eng.*, **110**(1), 73-78.

Keyhani, R. and Haeri, S.M. (2013), "Evaluation of the effect of anisotropic consolidation and principle stress rotation on undrained behavior of silty sands", *Scientia Iranica A*, **20**(6), 1637-1653.

Newmark, N.M. (1935), "Simplified computation of vertical pressures in elastic foundations", *Circular No. 24*, University of Illinois Engineering Experiment Station, IL, USA.

Poulos, H.G. and Davis, E.H. (1974), *Elastic Solutions for Soil and Rock Mechanics*, John Wiley and Sons, Inc.

Rahhal, M.E. and Lefebvre, G. (2000), "Understanding the effect of a static driving shear stress on the liquefaction resistance of medium dense granular soils", *Soil Dyn. Earthq. Eng.*, **20**(5-8), 397-404.

Seed, H.B. (1983), "Earthquake resistant design of earth dams", *Proceedings of Symposium on Seismic Design of Embankments and Caverns*, *ASCE*, pp. 41-64.

Sivathayalan, S. and Ha, D. (2011), "Effect of static shear stress on the cyclic resistance of sands in simple shear loading", *Can. Geotech. J.*, **48**(10), 1471-1484.

Song, B.W. (2003), "The influence of initial static shear stress on post-cyclic degradation of non-plastic silt", *Lowland Technol. Int.*, **5**(1), 14-24.

Stoll, U.W. (1960), "Computer solution of pressure distribution problem", *J. Soil Mech. Found. Div.*, **86**(6), 1-9.

Uchida, K. and Hasegawa, T. (1986), "Strength-deformation characteristics of a soil subjected to initial shear stress", *Soils Found.*, **26**(1), 11-24.

Vaid, Y.P. and Chern, J.C. (1983), "Effect of static shear on resistance to liquefaction", *Soils Found.*, **23**(1), 47-60.

Vaid Y.P., Stedman, J.D. and Sivathayalan, S. (2001), "Confining stress and static shear effects in cyclic liquefaction", *Can. Geotech. J.*, **38**(3), 580-591.

Vitone, D.M.A. and Valsangkar, A.J. (1986), "Stresses from loads over rectangular areas", *J. Geotech. Eng.*, **112**(10), 961-964.

Wang, C.D. and Liao, J.J. (2002), "Elastic solutions for stresses in a transversely isotropic half-space subjected to three-dimensional buried parabolic rectangular loads", *Int. J. Numer. Anal. Method. Geomech.*, **26**(14), 1449-1476.

Yang, J. and Sze, H.Y. (2011), "Cyclic behavior and resistance of saturated sand under non-symmetrical loading conditions", *Geotechnique*, **61**(1), 59-73.

Yang, J., Sze, H.Y., Heung, M.K. and Wang, G.H. (2013), "On correction factors for liquefaction analysis of embankments and slopes", *Geotechnical Special Publication*, **231**, 850-853.

CC